

PREDICTION OF DESTABILIZING BLADE TIP FORCES

FOR SHROUDED AND UNSHROUDED TURBINES*

Yuan J. Qiu and M. Martinez-Sanchez
 Massachusetts Institute of Technology
 Cambridge, Massachusetts 02139

Highly loaded turbomachinery tends to exhibit noticeable subsynchronous whirl at a frequency close to one of the rotor critical frequencies when the rotating speed is well in excess of that critical. The subsynchronous whirl is not a "forced" vibration phenomenon where the vibration frequency is the same as the forcing frequency; e.g., rotor unbalancing. It is better classified as a positive feedback phenomenon tending to amplify small disturbances at the system natural frequencies. The cause of whirl can be traced back to a number of forcing mechanisms. One of these is the variation of the blade tip forces due to nonuniform blade tip clearance. Alford (1) was the first to model this aerodynamic force on the blade. By assuming uniform upstream and downstream flow fields, he was able to argue that the variation of the blade tip force would be proportional to the efficiency variation. Therefore, if a turbine rotor has some small eccentricity (Fig. 1), then due to the efficiency variation, the blade force on the narrow-gap side must be greater than the blade force on the opposite side. The resultant force F_y on the rotor, acting perpendicular to the eccentricity is then not zero. This force can cause the rotor to whirl forward, i.e., in the same direction as the rotation. Qualitatively:

if

$$\frac{\delta \eta}{\eta_m} = \beta \frac{\delta t}{H}, \quad \delta t = e_o \cos \theta$$

then

$$F_y = \frac{T_m \beta}{D_m} \frac{e_o}{H}$$

where δt is the local tip clearance at azimuth θ , e_o is the eccentricity and H is the blade height, D_m is the mean diameter of the rotor and T_m is torque on the rotor, β is a numerical factor of order unity depending on the blading.

Contrary to Alford's assumptions, the presence of the blade tip clearance variation is bound to influence the whole flow field. The purpose of this paper is to investigate the effect of this non-uniform flow field on the Alford force calculation. The ideas used here are based on those developed by Horlock and

* This work was supported by NASA contract NAS8-35018.

Greitzer (2). It will be shown that the non-uniformity of the flow field does contribute to the Alford force calculation. An attempt is also made to include the effect of whirl speed. The values predicted by the model are compared with those obtained experimentally by Urlicks(3) and Wohlrab (4). The possibility of using existing turbine tip loss correlations to predict β is also exploited.

The Model

The method of approach is to first find the flow field due to the tip clearance variation, and then, using the velocity triangles, to calculate the resultant Alford force. The detail of the analysis is given in Ref. 5. It is to be stressed that a complete three-dimensional investigation of the flow field with the non-uniform tip clearance is not attempted here.

Consider a single-stage turbine with its rotor whirling at a constant eccentricity e_0 (Fig. 2). If the hub/tip ratio is high, the flow field can be approximated to be two dimensional. Fig.3 shows an actuator disc representing a two dimensional unwrapped blade row of circumference $2\pi R$, where w is the relative flow velocity and c is the absolute flow velocity. If the Mach numbers upstream and downstream are small, the flow can be considered incompressible, as well as inviscid, outside of the blade row.

The variation of the tip clearance around the annulus can be represented by

$$\delta \frac{t}{H} = \sum E_n \left[i \frac{y}{R} n - \Omega t i \right] \quad (1)$$

where Ω is the whirling speed, y is the distance in the tangential direction, R is the mean blade radius, H the blade height, and the E_n are constants.

Since only the first harmonic is of interest, as will be explained later, higher harmonics are not included in the analysis and $E_1 = e_0/H$.

The perturbation velocities c'_x and c'_y are related to the stream function ψ by

$$c'_x = \frac{\partial \psi}{\partial y} \quad (2a)$$

$$c'_y = - \frac{\partial \psi}{\partial x} \quad (2b)$$

Upstream of the stage, the flow is irrotational, $\nabla^2 \psi_1 = 0$ and downstream the flow is rotational $\nabla^2 \psi_2 = \zeta$. The flow is steady in a reference frame rotating at the whirl speed Ω , therefore the stream functions can be written as

$$\psi_1 = A \exp \left[\frac{1}{R} (x + i y) - \Omega t i \right] \quad \text{upstream of the stage} \quad (3)$$

$$\psi_3 = B \exp \left[\frac{1}{R} (-x + iy) - \Omega t \right] + C \exp \left[\frac{1}{R} (-x \tan \bar{\alpha}_3 i + y i - \Omega t) \right] \text{ downstream of the stage} \quad (4)$$

where $\bar{\alpha}_3$ is the mean flow angle downstream of the rotor. Notice the irrotational term dies out far upstream and downstream. The vorticity downstream is convected by the mean flow at an angle $\bar{\alpha}_3$. Again only first harmonics are considered.

There are three matching conditions across the actuator disc surface:

- 1) The axial mass flux is constant

$$c'_{x1} = c'_{x3} \quad (5)$$

or

$$\frac{\partial \psi_1}{\partial y} (0, y) = \frac{\partial \psi_3}{\partial y} (0, y)$$

- 2) The relative flow leaving angle is constant

$$\tan \beta_3 c'_{3x} = w'_{3x} = c'_{3y} + u' \quad (6)$$

at $x = 0$

- 3) The third boundary condition involves matching perturbation quantities by using the known experimental information.

The total-to-static turbine efficiency can be written as

$$\eta = \frac{(c_{y3} - c_{y2}) u}{c_p T_{01} \left(1 - \left(\frac{p_3}{p_{01}} \right)^{\frac{\gamma-1}{\gamma}} \right)} = \frac{\text{turbine work}}{\text{ideal work}} \quad (7)$$

where c_{y2} and c_{y3} are the y-components of the absolute flow velocity before and after the rotor (defined positive in the y direction), u is the blade speed, p_3 is the static pressure downstream of the disc, and p_{01} is the total pressure upstream.

Due to the local blade tip clearance variation, the efficiency can be written as the sum of the mean efficiency and its perturbation:

$$\eta = \bar{\eta} + \eta' \quad (8)$$

where to a first approximation

$$\eta' = \frac{\partial \bar{\eta}}{\partial (t/H)} \delta (t/H) + \frac{\partial \bar{\eta}}{\partial \beta_1} \delta \beta_1 \quad (9)$$

It is known that the second term in the above expression is small compared with the first term, if β is not too far from the designed value. Hence the second term in Eq.(9) will be ignored in the analysis.

We now perturb eq.(7) and use the additional condition that the stator leaving angle is also constant to eliminate c_{y2} , the third boundary condition is obtained. We also use the downstream y -momentum equation to eliminate the downstream pressure perturbation. In terms of the perturbation streamfunctions, the three matching conditions can then be written as

$$\frac{\partial \psi_1}{\partial y} = \frac{\partial \psi_3}{\partial y}$$

$$\frac{\partial \psi_3}{\partial y} \tan \beta_3 = - \frac{\partial \psi_3}{\partial x} + u'$$

$$\begin{aligned} \frac{\partial \eta'}{\partial y} \bar{Q}_1 + \bar{Q}_2 \rho_3 \left[\bar{c}_{x3} \frac{\partial^2 \psi_3}{\partial x \partial y} + \bar{c}_{y3} \frac{\partial^2 \psi_3}{\partial y \partial x} + \frac{\partial^2 \psi_3}{\partial t \partial x} \right] \\ = - u \left[\frac{\partial^2 \psi_3}{\partial x \partial y} + \tan \alpha_2 \frac{\partial^2 \psi_1}{\partial y^2} \right] + (c_{y3} - c_{y2}) \frac{\partial u'}{\partial y} \end{aligned} \quad (10)$$

where

$$\bar{Q}_1 = \left[\begin{array}{c} (\gamma-1)/\gamma \\ c_{pT01} \left(1 - \frac{p_3}{p_{01}} \right) \end{array} \right]; \quad \bar{Q}_2 = \left[\begin{array}{c} (\gamma-1)/\gamma \\ - \eta \frac{c_{pT01}}{p_3} \frac{\gamma-1}{\gamma} \left(\frac{p_3}{p_{01}} \right) \end{array} \right]$$

Substituting the forms given by Eqs. (3) and (4) for ψ_1 and ψ_3 , these conditions become three linear algebraic equations for the coefficients A, B and C. To obtain the blade force variation, the momentum equation is applied across the rotor blades. The tangential component of the force is given by

$$f_Y = \rho c_{x3} (c_{y3} - c_{y2}) H \quad (11)$$

Since only the perturbation of force contributes to the resultant destabilizing force

$$f_Y' = \rho c_{x1} (\bar{c}_{y3} - \bar{c}_{y2}) H + \rho_1 \bar{c}_x (c_{y3}' - c_{y2}') H \quad (12)$$

If we consider a reference frame rotating at the whirl speed Ω , and add together the forces perpendicular to the instantaneous eccentricity, we find the net cross-force

$$F_Y = \int_0^{2\pi R} \text{Real}(f_Y' e^{\Omega t}) \cos(\gamma/R) d\gamma \quad (13)$$

This expression justifies the inclusion of only the first harmonic in the stream function expansion, since the higher harmonics contribute nothing to the Alford force. A non-dimensional excitation coefficient k_{xy} is defined as

$$k_{xy} = \frac{F_y}{U_s} / \frac{e_0}{H} \quad (14)$$

where U_s is the ideal total force in the circumferential direction on the blade, and e_0/H is the dimensionless eccentricity.

Results

Cases with stationary eccentricity are considered first. A typical plot of the axial velocity perturbation and the blade force variation vs. angular position are shown in Fig. 4. As was to be expected, these quantities are almost in counterphase with the tip clearance variation, which indicates that the nonuniform flow field will tend to increase the Alford forces.

Although Alford published his paper in 1965, very few experiments have been done to verify the proposed formula. Hence it is difficult to make any good comparison between the Alford model, the present analysis, and experimental results. Two tests were done by Urlich (3) and Wolhrab (4), and more recently Vance and Laudadio (6) did verify the linearity between the Alford forces and eccentricity for a fan. Accurate experimental data seems very difficult to obtain due to the small magnitude of the forces to be measured.

For the present analysis the data of Urlich seems to be the more suitable, since he also determined the efficiency vs. average clearance for an unshrouded turbine stage. From this information the values of $\lambda = \partial\eta/\partial(t/H)$ are found by a second order polynomial curve fit to the efficiency vs. clearance data (Table 1). Values of k_{xy} are found by using λ , together with appropriate flow angles (Ref. 3) in the analytical model. The predicted values and experimentally obtained values of k_{xy} are plotted in Figs. 5 and 6, together with the values of k_{xy} obtained from the Alford formula. It can be seen that the analysis gives a value of k_{xy} higher than the Alford formula, indicating that the non-uniformity does increase the destabilizing forces.

In addition, it is also clear from Figs. 5 and 6 that the new theory overpredicts the side forces, when compared to the experimental data. However, we should at this point also consider the effect of the nonuniform pattern of pressure acting on the turbine wheel rim. Fig. 7 shows that, although the pressure field just upstream of the rotor is in phase with the clearance variation, it is shifted by 90° just downstream, and that those nonuniform pressures act in such a way as to reduce the forward cross-force.

A precise accounting of the effect of these pressure forces is not possible in the context of our actuator-disc theory. However, we can see that the 90° rotation of the pressure pattern must occur in the rotor passages, and so it is logical to calculate the induced side force by letting the rotated pressure wave act on an axial rim width equal to half a blade chord. New excitation coefficients, including this pressure force, are also shown in Fig. 6. Although the precise axial length over which the pressure forces act is difficult to determine, it can be seen that they do contribute significantly to the net force, and that their effect is to essentially remove the overprediction.

The Use of Tip Clearance Correlations

In many situations, curves of efficiency vs. clearance are not available. The possibility of using some of the existing tip clearance loss correlations is investigated here. The formula used is given by Dunham and Came (7), in the form of a tip loss coefficient which depends on flow angles and other stage variables, as well as on the clearance to chord ratio. This allows determination of η , and hence λ for use in our model. Fig. 8 shows the predicted Alford forces based on the tip loss clearance correlation(Ref.(7)), together with the experimental results. It can be seen that the prediction is very reasonable, as it compares well with the data for small axial (stator-rotor) gap, although not as well for large axial gap. The fact that k_{xy} varies with the gap between the rotor and stator is not well understood, and it may be highly dependent on the detailed geometrical arrangement of stator and rotor.

Wohlrab (Ref. 4) tested a shrouded turbine. Since he did not supply data on efficiency vs. tip clearance, λ has to be estimated, in order to compare the present analysis with the experimental values obtained. Encouraged by the results for the unshrouded turbine, an estimated tip loss coefficient is used again, but this time the effective tip clearance is given by (Ref.(7)).

$$t = (\text{geometric tip clearance}) \times (\text{number of seals})^{-0.42}$$

Since there is also a shroud, we would expect some seal forces acting on the rotor shroud band. These are found by applying a model developed by Lee, et al. (8). The results (Fig. 9) again show reasonable agreement, falling between the data obtained by Wohlrab for the two axial gaps tested.

Effect of Whirl

All the cases examined so far have been for an assumed static offset. The effect of whirl for a typical case is shown in Fig. 10. For a whirl speed equal to 50% of the rotating speed, the effect on k is small ($\pm 10\%$). This is consistent with Wohlrab's experiment, in which he found that within experimental accuracy there is no difference between the values of k_{xy} obtained from kinetic and static tests. It is noted, however, that the predicted effect of whirl (which could be expressed as an Alford damping coefficient), could not have been obtained from the original Alford model, since it depends crucially on the delays between wheel motion and disc passage of the induced flow non-uniformities, and these were ignored in the Alford model.

Conclusion

The non-uniform flow field induced by the tip clearance variation tends to increase the resultant destabilizing force over and above what would be predicted on the basis of the local variation of efficiency. On the one hand, the pressure force due to the non-uniform inlet and exit pressure also plays a part even for unshrouded blades, and this counteracts the flow field effects, so that the simple Alford prediction remains a reasonable approximation. Once the efficiency variation with clearance is known, the present model gives a slightly overpredicted, but reasonably accurate destabilizing force. In the absence of efficiency vs. clearance data, an empirical tip loss coefficient can be used to give a reasonable prediction of destabilizing force. To a first approximation, the whirl does have a damping effect, but only of small magnitude, and thus it can be ignored for some purposes. To gain more insight and understanding, more accurate

experimental determinations of the tip force must be made. It must be pointed out that the destabilizing force is also highly dependent on the geometry of the rotor and stator, as shown by the experimental dependence of the magnitude of destabilizing force on the axial gap between the stator and rotor. This effect of axial gap on the Alford force points to the need for more detailed study of the flow field around tip regions.

References

1. Alford, E.F., "Protecting Turbomachinery from Self-Excited Rotor Whirl." Journal of Engineering for Power, Oct. 1965, pp338-344.
2. Horlock, J.H. and Greitzer, E.M., "Non-uniform Flows in Axial Compressors Due to Tip Clearance Variation," Proc. Instn. Mechanical Engrs., Vol. 197c, pp173
3. Urlichs, K., Clearance Flow Generated Transverse Force at the Rotors of Thermo Turbomachines," Dissertation, Technical University of Munich, (1975). English translation in NASA TM-77 292, Oct. 1983.
4. Wohlrab, R., "Experimental Determination of Gap Flow-Conditioned Force at Turbine Stages and Their Effect on the Running Stability of Simple Rotors," Dissertation, Munich Institute of Technology (1975). English translation in NASA TM-77 293, Oct. 1983.
5. Martinez-Sanchez, M, Greitzer, E. and Qiu, Y., "Turbine Blade-Tip Clearance Excitation Forces," Report on NASA Contract Number NAS8-35018, June, 1985.
6. Vance and Laudadio, "Experimental Measurement of Alford's Force in Axial Flow Turbomachinery," Journal of Engineering for Gas Turbines and Power, 1984, pp585.
7. Dunham and Came, "Improvements to the Ainley-Mathieson Method of Turbine Performance Prediction," ASME Transactions, July 1970.
8. Lee, D.W.K., Martinez-Sanchez, M. and Czajkowski, E., "The Prediction of Force Coefficients for Labyrinth Seals," 3rd Rotordynamic Instability Workshop, Texas A&M University, May 1984.

List of Symbols

c	absolute velocity
c_p	specific heat
D_m	mean rotor diameter
e_0	eccentricity
f_y	blade force per unit circumferential length
F_y	tangential force
H	blade span
K_{xy}	excitation coefficient
p	pressure

R blade radius
 t time; tip clearance
 T temperature
 T_m mean torque on rotor
 w relative velocity
 u blade speed
 U_s ideal blade force=(ideal turbine work)/(blade speed)
 α absolute flow angle
 $\beta_{1,2,3}$ relative flow angle
 β Alford factor
 ζ perturbation vorticity
 θ circumferential angle
 Ψ stream function
 Ω whirl speed
 ρ density
 η efficiency

Superscript

' perturbation
 - mean value

subscript

y tangential direction
 x axial direction
 1 upstream of stator
 2 downstream of stator
 3 downstream of rotor
 0 stagnation

	radial	clearance / blade height	
	2.6 %	5.3 %	7.8 %
axial gap 7.1 %	.705	.594	.521
21 %	.716	.570	.440

Table.1 Efficiency for tip clearances

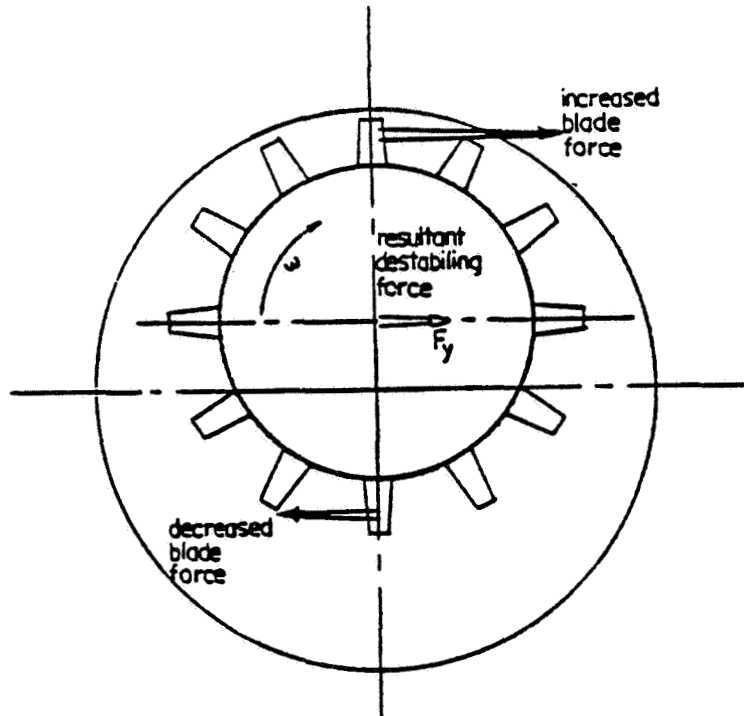


Figure 1. - Tip clearance effect for turbine rotor.

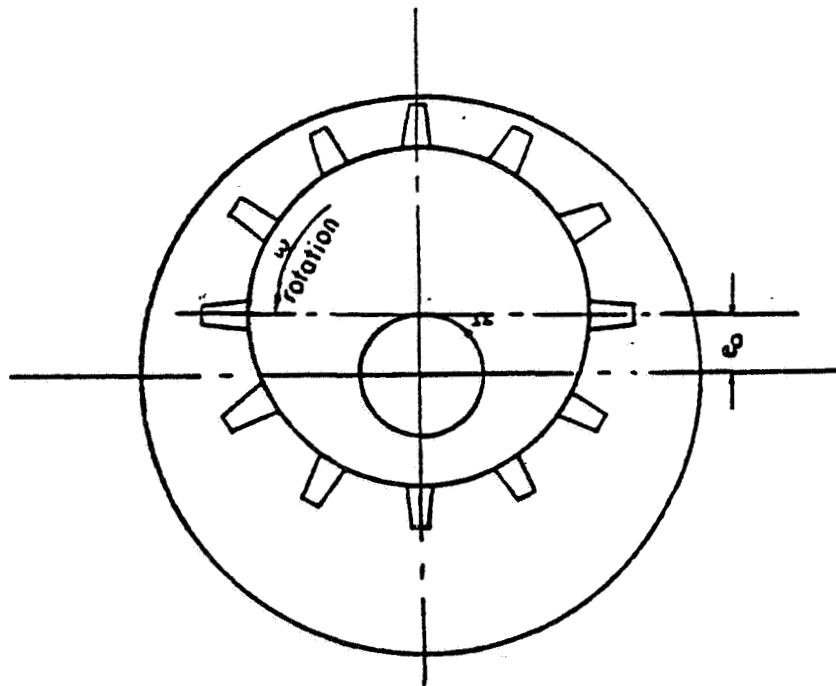


Figure 2. - Rotor under whirl.

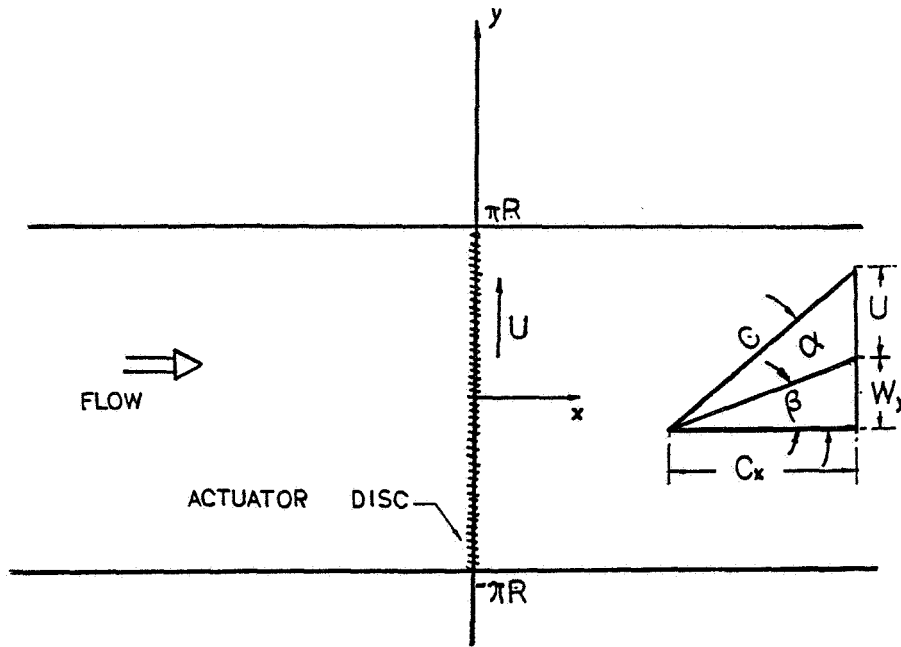


Figure 3. - Two-dimensional flow model.

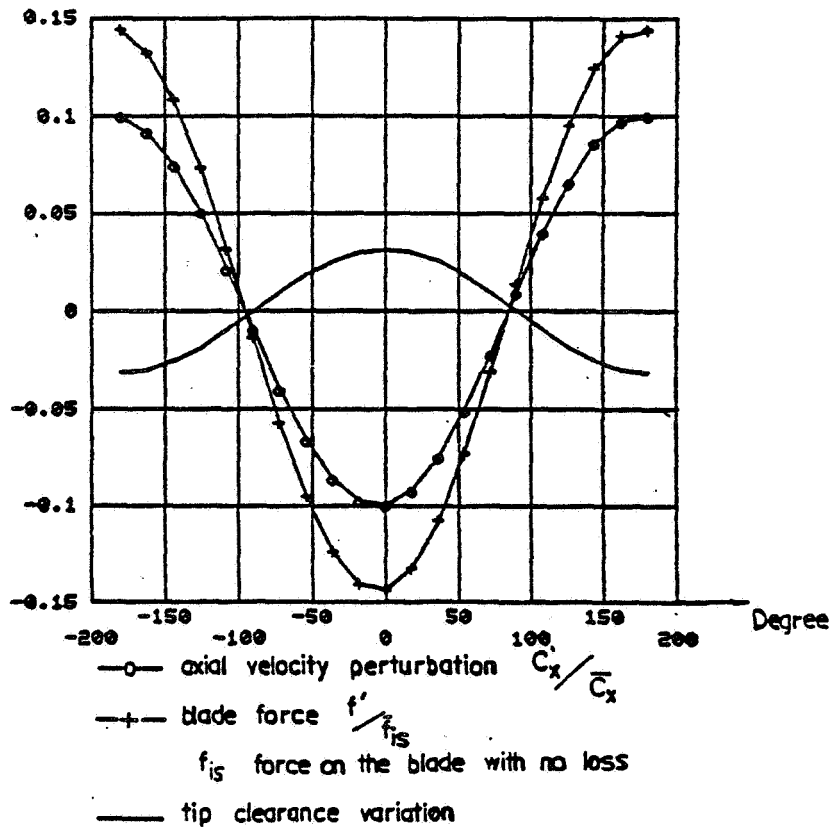


Figure 4. - Axial velocity and local blade force distribution.

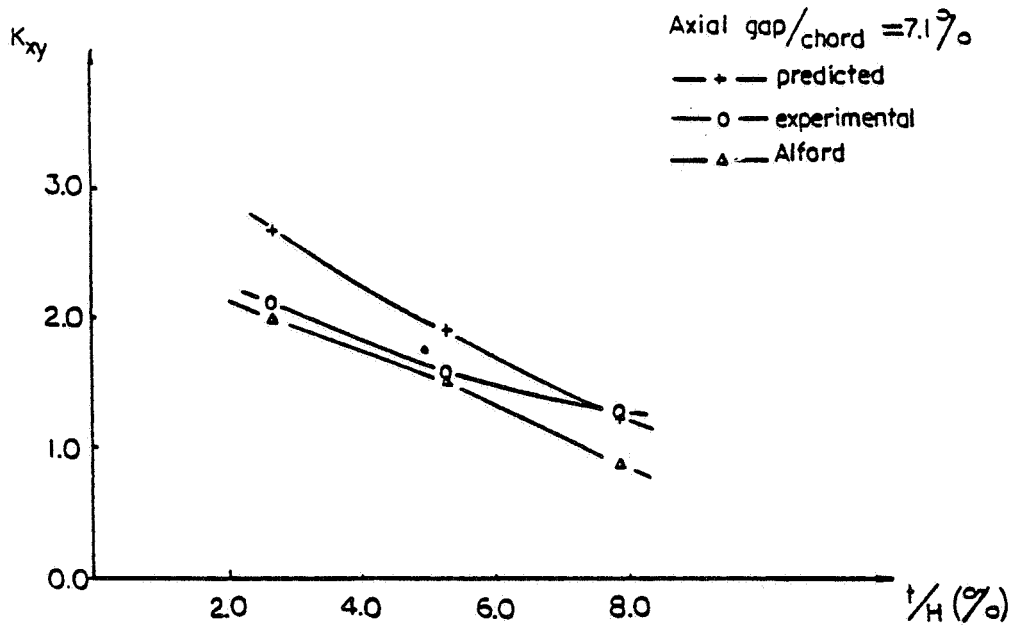


Figure 5. - Variation of excitation coefficient with tip clearance.

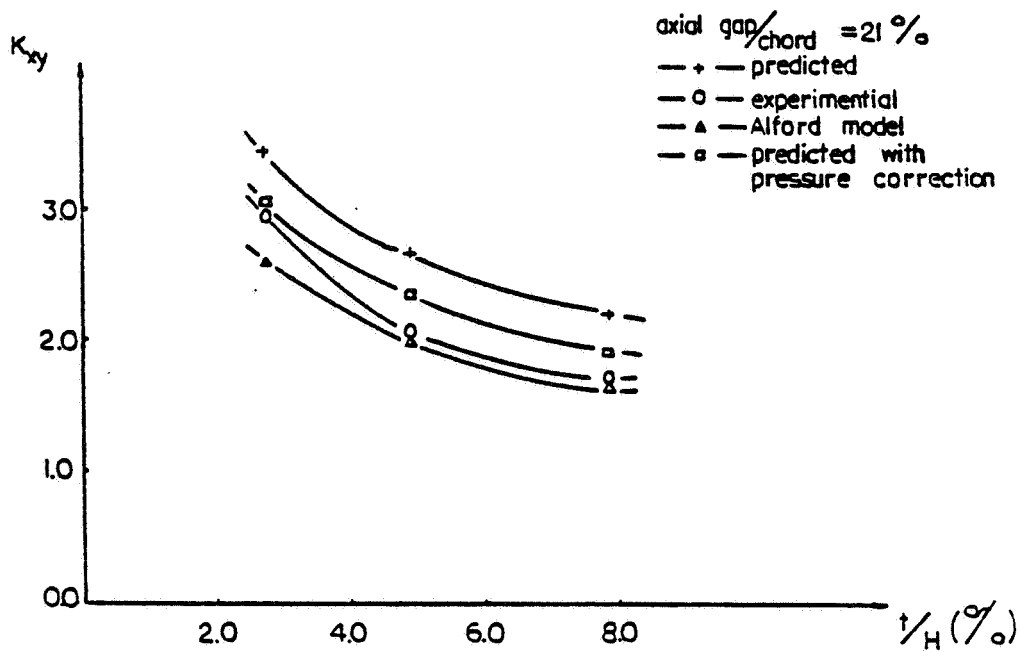


Figure 6. - Variation of excitation coefficient with tip clearance.

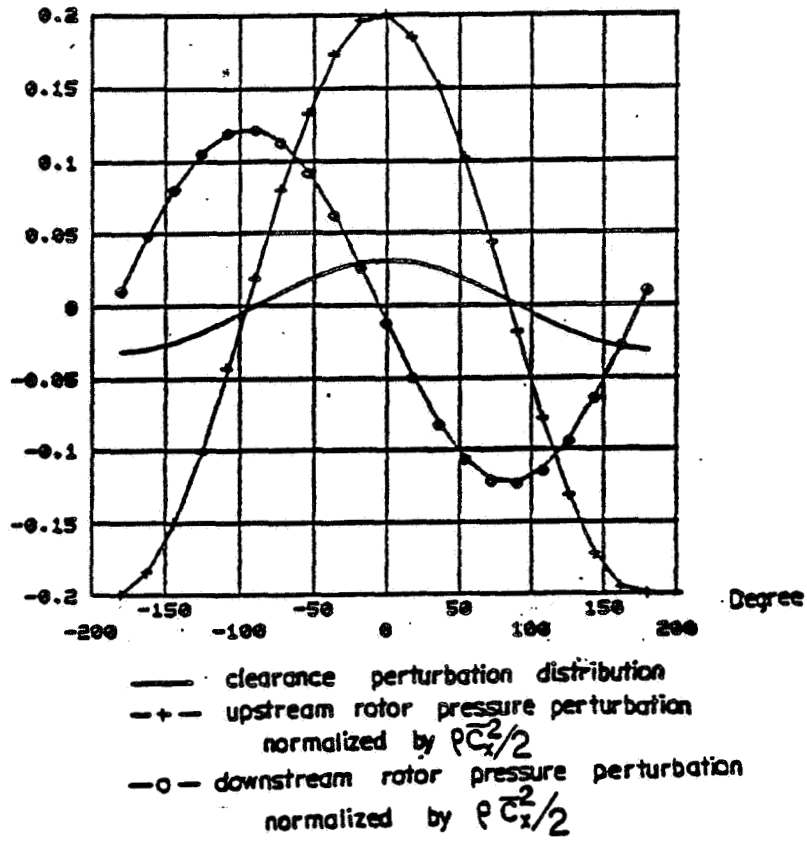


Figure 7. - Pressure perturbation distribution.

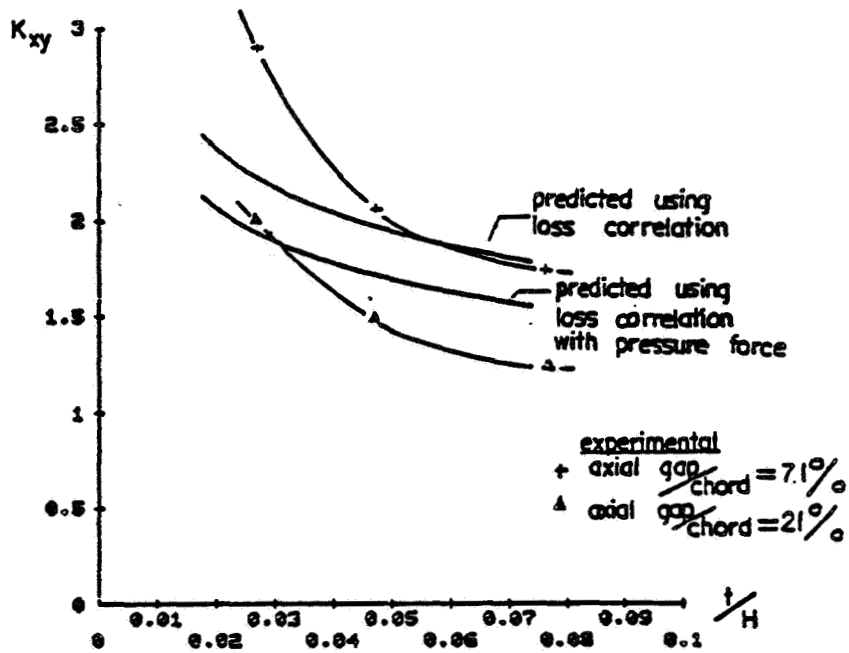


Figure 8. - Variation of excitation coefficient with tip clearance.

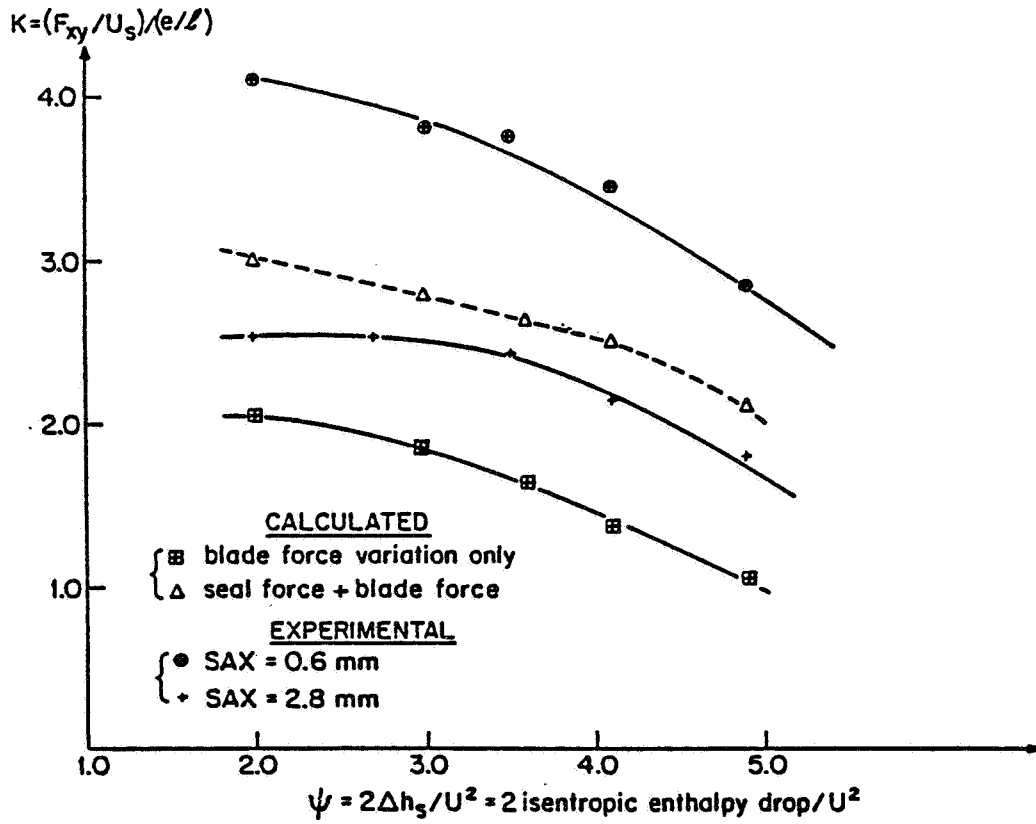


Figure 9. - Variation of clearance excitation coefficient with ψ .

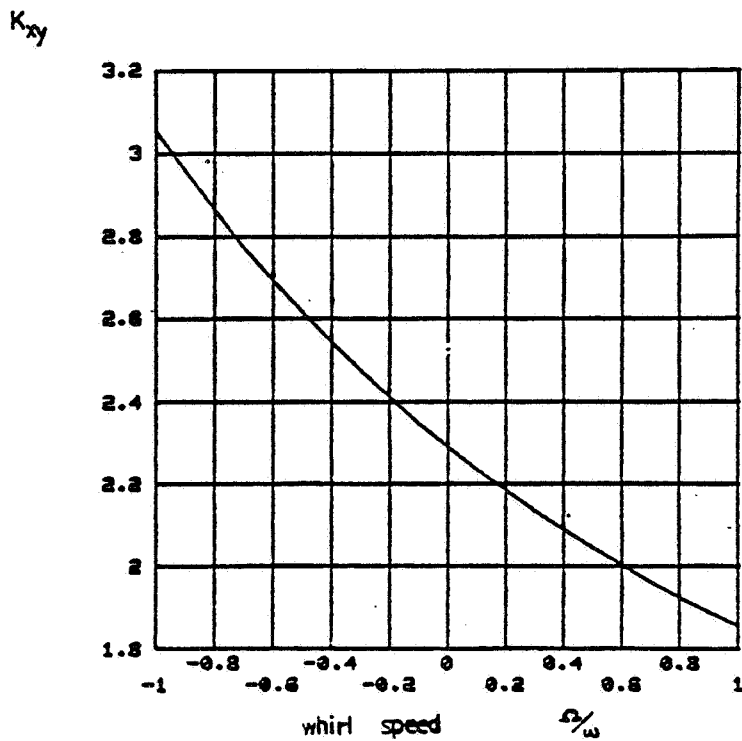


Figure 10. - Effect of whirl.